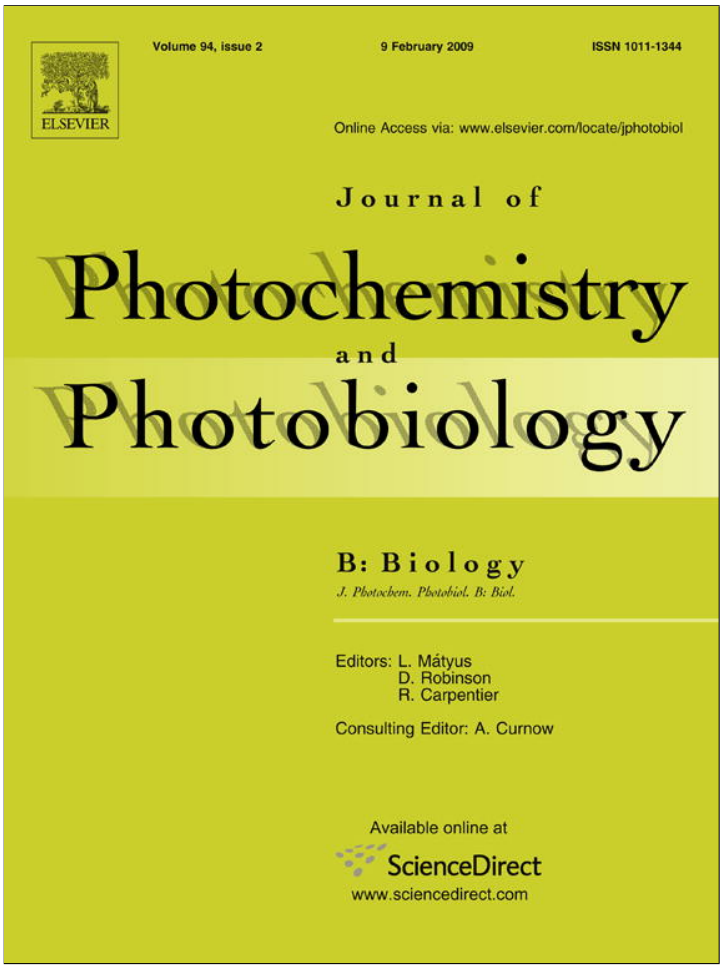

Journal of Photochemistry and Photobiology B: Biology 94 (2009) 82–86

Contents lists available at ScienceDirect

Journal of Photochemistry and Photobiology B: Biology

journal homepage: www.elsevier.com/locate/jphotobiol

Responses of a marine red tide alga *Skeletonema costatum* (Bacillariophyceae) to long-term UV radiation exposures

Hongyan Wu [a,*], Kunshan Gao [b], Haiyan Wu [a]

[a] Marine Biology Institute, Shantou University, No. 243 Daxue Road, Shantou, Guangdong 515063, China
[b] State Key Laboratory of Marine Environmental Science, Xiamen University, Xiamen 361005, China

ARTICLE INFO

Article history:
Received 30 April 2008
Received in revised form 18 October 2008
Accepted 21 October 2008
Available online 26 October 2008

Keywords:
Growth rate
Photosynthesis
UV
UV-absorbing compounds
Skeletonema costatum

ABSTRACT

UV radiation (280–400 nm) is known to affect phytoplankton in negative, neutral and positive ways depending on the species or levels of irradiation energy. However, little has been documented on how photosynthetic physiology and growth of red tide alga respond to UVR in a long-term period. We exposed the cells of the marine red tide diatom *Skeletonema costatum* for 6 days to simulated solar radiations with UV-A (320–400 nm) or UV-A + UV-B (295–400 nm) and examined their changes in photosynthesis and growth. Presence of UV-B continuously reduced the effective photosynthetic quantum yield of PSII, and resulted in complete growth inhibition and death of cells. When UV-B or UV-B + UV-A was screened off, the growth rate decreased initially but regained thereafter. UV-absorbing compounds and carotenoids increased in response to the exposures with UVR. However, mechanisms for photoprotection associated with the increased carotenoids or UV-absorbing compounds were not adequate under the continuous exposure to a constant level of UV-B (0.09 W m^{-2}, DNA-weighted). In contrast, under solar radiation screened off UV-B, the photoprotection was first accomplished by an initial increase of carotenoids and a later increase in UV-absorbing compounds. The overall response of this red tide alga to prolonged UV exposures indicates that *S. costatum* is a UV-B-sensitive species and increased UV-B irradiance would influence the formation of its blooms.

1. Introduction

Enhanced solar UV-B radiation reaching the Earth's surface due to thinning of the stratospheric ozone layer can result in significant impacts on various organisms [1]. Increased UV-B radiation has been found to be detrimental to all kinds of photosynthetic organisms by affecting a number of physiological and biochemical processes, such as growth, pigmentation, enzymes and photosynthesis [2–5]. Most commonly, studies on phytoplankton have examined short-term (a few hours) effects on photosynthesis and DNA [6,7]. These results are important to look at the initial responses to UV stress, however, they can hardly reflect the effects over long-term exposures. Further damages [8–10] or acclimation [11,12] might occur over longer periods (days) of exposure. Since red tides always sustained for several days, long-term studies (>1 d) seemed required to examine the responses of red tide alga to solar UVR. In addition, photoprotective strategies developed to minimize UVR-related harms [13,14], such as synthesis of UV-absorbing compounds (mainly mycosporine-like amino acids (MAAs)) or production of quenching agents, can be accomplished in different time scales for different species or radiation treatments. Therefore, long-term studies are needed to elucidate the balance between damage and repair when cells are considered for their sensitivity to UVR.

Skeletonema costatum is a cosmopolitan marine diatom and known as a major component of most red tides in eutrophic regions [15,16], causing huge economic loss in aquaculture, though it is also used as a food organism. Many studies had focused on the ecophysiology of *S. costatum*, especially on its carbon acquisition mechanisms in relation to CO_2 levels in the context of red tide [17–21]. However, *S. costatum* is inevitably exposed to high solar UV radiation when it forms red tide with cells concentrated to the upper water layers. A few studies, using UV-B lamp in a short-time scale, showed that UV-B radiation could damage the DNA in *S. costatum* [22,23] and influence its ability of competition with other species [24]. Recently, it has been shown that light history affected the physiological responses of *S. costatum* to solar UVR [25]. Nevertheless, our knowledge about the physiological behavior of *S. costatum* in the presence of UVR is still limited.

In the present study, we investigated the effects of prolonged UV exposure on growth rate, cell size and photosynthesis of the red tide alga *S. costatum*, and also examined the mechanisms by which this organism cope with UVR.

* Corresponding author. Tel./fax: +86 754 2903977.
E-mail address: wuhy@stu.edu.cn (H. Wu).

1011-1344/$ - see front matter © 2008 Elsevier B.V. All rights reserved.
doi:10.1016/j.jphotobiol.2008.10.005

2. Materials and methods

2.1. Organisms

Skeletonema costatum (Greville) Cleve (strain 2042) was obtained from the Institute of Oceanography, the Chinese Academy of Sciences, and maintained under axenic conditions in the laboratory. The cells were grown in filtered and sterilized seawater enriched with f/2 medium under 200 μmol m^{-2} s^{-1} (12:12 LD cycle) at 20 °C before being used for experiments.

2.2. UV radiation treatments

Cells at mid-exponential growth phase were harvested, washed once and resuspended in fresh media to a final concentration of about 1×10^6 cells mL^{-1}. They were dispensed in UV-transparent quartz tubes, which were maintained in a flowthrough water bath for temperature control at 20 ± 1 °C. The cultures were aerated (0.3 L min^{-1}) and exposed to three different radiation treatments: (1) cells receiving UV-B, UV-A and PAR (PAB treatment, 295–700 nm) – quartz tubes covered with Ultraphan film 295 (UV Opak, Digefra, Munich, Germany); (2) cells receiving UV-A and PAR (PA treatment, 320–700 nm) – quartz tubes covered with Folex 320 (Montagefolie, No. 10155099, Folex, Dreieich, Germany) and; (3) cells receiving PAR alone (P treatment, 395–700 nm) – quartz tubes covered with Ultraphan film 395 (UV Opak, Digefra, Munich, Germany). The irradiance of PAR was set at 788.9 μmol m^{-2} s^{-1} (161 W m^{-2}), UV-A and UV-B were at 28 and 0.9 W m^{-2}, respectively. DNA-weighted UV-B irradiance was 0.09 W m^{-2} [26]. Such irradiance levels were based on the averaged daytime solar irradiances for each band measured locally in May and June when the red tide organism bursts out with high frequency. The constant levels of PAR, UV-A and UV-B were provided for 12 h every 24 h (12 h darkness) with a solar simulator (Sol 1200, Dr. Hönle GmbH, Germany) equipped with a 1000-W xenon arc lamp and were measured with a broadband filter radiometer (ELDONET, Real Time Computer Inc., Germany).

The cultures were operated semi-continuously by renewing partially the medium every 24 h to the initial cell concentration except for those under PAB treatment that caused cell death due to the lethal effects of UV-B. Samples were taken from each radiation treatment every day at the middle of the light period (6 h) to determine effective quantum yield of PSII, cell concentration, concentration of UV-absorbing compounds and photosynthetic pigments.

2.3. Morphological examination and cell count

Morphological examinations were performed using a compound microscope (Zeiss Axioplan 2, Carl Zeiss Germany). Digital images were recorded with a Zeiss Axicam camera and analyzed with a Vision Analysis System (AxioVision 3.0). Length axes (l) and diameter (d) of 100–200 cells were measured in at least 10 fields. The means of l and d were used to calculate cell volume of the cylindrical diatom as: $\pi \times (d/2)^2 \times l$ [27]. Cells were counted microscopically using a haemacytometer.

2.4. Growth rates

Samples were taken daily for cell counts and the specific growth rate (μ) was calculated as

$$\mu = \ln(X_n/X_{n-1})/(T_n - T_{n-1}),$$

where X_n and X_{n-1} are the cell concentrations (cells ml^{-1}) at the beginning and end of (T_n–T_{n-1}) period.

2.5. Measurements of effective quantum yield

A portable pulse amplitude modulated fluorometer (PAM-WATER-ED, Walz, Germany) was used to determine the chlorophyll fluorescence. The effective photosynthetic quantum yield (Φ_{PSII}) was determined by measuring the instant maximal fluorescence (F'_m) and the steady state fluorescence (F_t) of light-adapted cells and calculated according to Genty et al. [28]as: $\Phi_{PSII} = (F'_m - F_t)/F'_m$. In the course of measuring F'_m and F_t, the saturating pulse and actinic light were set at 4000 and 150 μmol m^{-2} s^{-1}, respectively.

UVR-induced inhibition of Φ_{PSII} was calculated as: Inh(%) = $(Y_P - Y_X) \times Y_P^{-1} \times 100$, where Y_P indicates the Φ_{PSII} under P treatment, while Y_X indicates that under either PA or PAB treatment.

2.6. Evaluation of UV-absorbing compounds and photosynthetic pigments

Samples were filtered onto Whatman GF/F glass fiber filters (25 mm). UV-absorbing compounds were extracted into 10 mL of absolute methanol overnight, centrifuged (5000*g* for 5 min) and the extract was scanned in the 250–750 nm wavelength interval using a scanning spectrophotometer (Shimadzu UV-1206, Japan). Total concentration of UV-absorbing compounds was estimated from the peak at 334 nm according to Dunlap et al. [29]. Chlorophyll *a* was extracted and determined according to Jeffrey and Humphrey [30]. The concentration of carotenoids (Car) was determined following the equations of Parsons and Strickland [31].

2.7. Statistical analysis

One-way analysis of variance and *t*-test were used to establish difference among the different radiation treatments. A confidence level of 95% was used in all analysis.

3. Results

Cell concentration of *S. costatum* in the cultures exposed to PAR + UV-A + UV-B (PAB) (Fig. 1A) decreased straightly from ca. 1×10^6 to 0.05×10^6 cells mL^{-1} by 20 times over a period of 6 days, indicating the complete inhibition of growth and death of cells. In contrast, cells receiving PAR or PAR + UV-A became acclimated after several days' exposure. The growth rate (μ) decreased till day 2 under PA and but till day 4 under the P treatment, then increased remarkably. Although presence of UV-A resulted in more

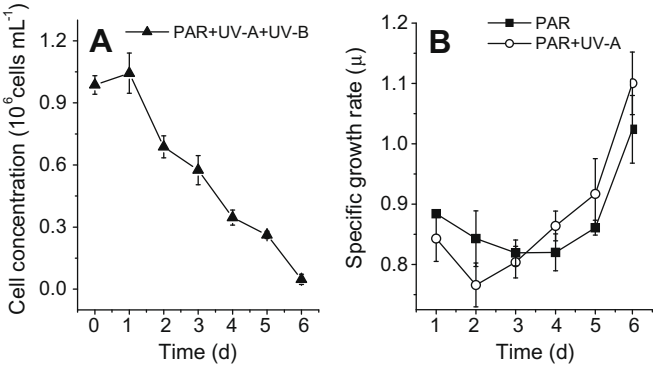

Fig. 1. Growth of *Skeletonema costatum* under different radiation treatments. (A) Changes in cell concentration under full-spectrum solar radiation (PAR + UV-A + UV-B: 295–700 nm) (n = 8); (B) specific growth rates under solar radiation depleted of UV-B (PAR + UV-A: 315–700 nm) and solar radiation deprived of total UV (PAR: 395–700 nm) (n = 3).

depression of the μ during the initial period, it led to faster recovery of the growth compared to the cells under PAR alone (Fig. 1B). However, there was no significant difference between PA and P treatments ($p > 0.05$).

Effects of different radiation treatments on the cell shape were shown in Fig. 2. There were no significant ($p > 0.05$) changes in the cell length axe and diameter under the PAB, PA and P treatments as compared with control (Fig. 2A). The average volumes of the cells were 3381(P), 3386(PA) and 3449(PAB) μm^3, respectively. Although it showed a slight increase of cell volumes under UV treatment in contrast with the control (3332 μm^3), no significant ($p > 0.05$) differences were found (Fig. 2B). Cell sizes were not affected by UV radiation.

The effective photosynthetic quantum yield (Φ_{PSII}) was also significantly inhibited by UV-B radiation (Fig. 3A). It was decreased to 28.7%, 48.8% and 62.8% of the initial value when exposed to PAB, PA and P treatments for 2 days, respectively. Prolonged exposure under PAB treatment resulted in further decline of Φ_{PSII}. It decreased to 17.5% of the initial value at the end of experimental period. While under PA and P treatments, Φ_{PSII} showed a recovery to the initial value after 6 days. When the inhibition of Φ_{PSII} by UV-B or UV-A was examined, respectively (Fig. 3B), it increased up to 84.7% with UV-B in 6 days, while for UV-A, it decreased with time as compared with the PAR treatment. At the end of the culture, after 6 days, UV-A resulted in positive effects (negative inhibition) by about 3%.

When the spectral characteristics of the *S. costatum* cells subjected to the PAB, PA and P treatments were compared (Fig. 4), an obvious absorption peak of UV-absorbing compounds (absorbance between 310 and 360 nm) was found in the cells exposed to PAB treatment. The absorptivity of these compounds increased significantly after 6 days exposure. In contrast, no absorption peak

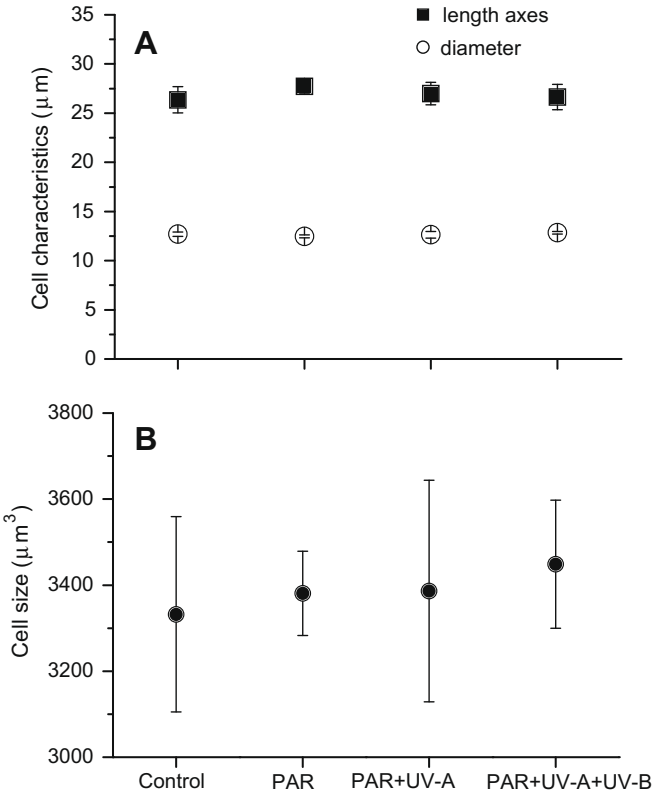

Fig. 2. Changes of the cell length axes, diameter (A) and cell size (B) in *Skeletonema costatum* exposed to solar irradiances under PAR, PAR + UV-A and PAR + UV-A + UV-B treatments for 6 days. (n = 100–200).

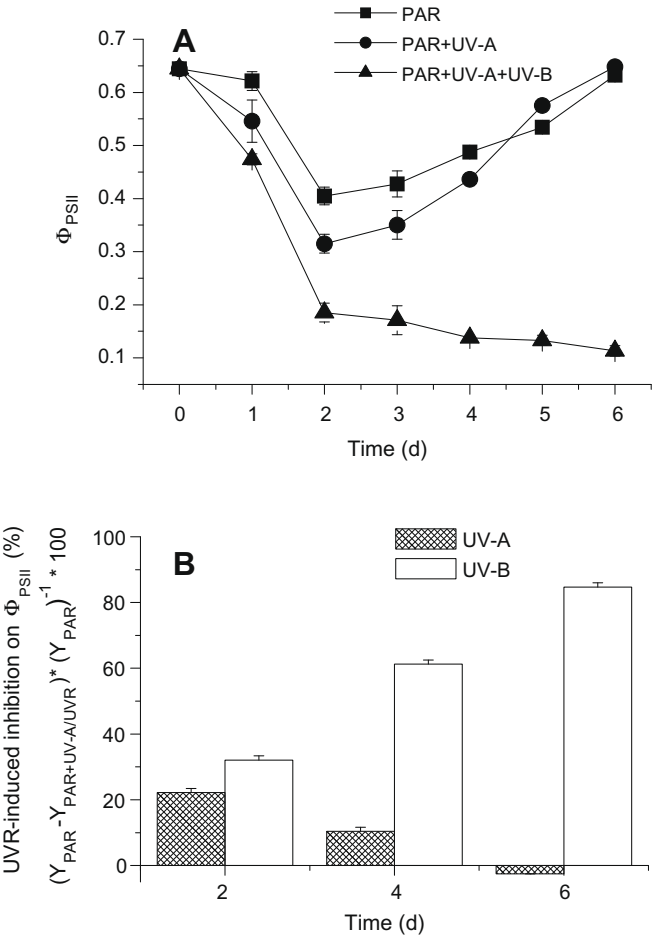

Fig. 3. Effective quantum yield of PSII (Φ_{PSII}) (A) and UVR-induced inhibition (B) for *Skeletonema costatum* cells exposed to solar irradiances for 6 days under PAR, PAR + UV-A and PAR + UV-A + UV-B treatments. The vertical lines indicate SD (n = 5).

was observed under PA and P treatments at day 3, and only a small peak was observed in 6 days. As shown in Table 1, the ratio of UV-absorbing compounds to Chl *a* under PAB treatment was about 10 times higher than that of under PA and P treatments after 6 days exposure. For the ratio of Car to Chl *a*, PAB treatment brought about the highest value of 0.77 at day 6, which was about 7 times higher

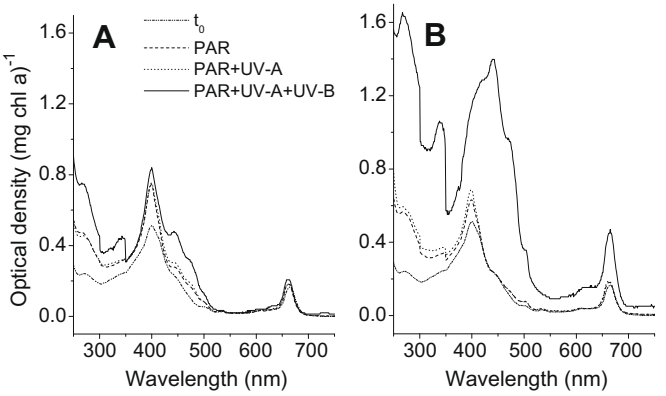

Fig. 4. Spectral characteristics of *Skeletonema costatum* exposed to solar irradiances under PAR, PAR + UV-A and PAR + UV-A + UV-B treatments. The ordinate is the optical density normalized to the concentration of chl *a*. A, samples exposed for 3 days; and B, samples exposed for 6 days.

Table 1
Ratios of UV-absorbing compounds and carotenoids (Car) to chlorophyll *a* (Chl *a*) in *Skeletonema costatum* cells exposed to PAR, PAR + UV-A, and PAR + UV-A + UV-B radiation for 3 and 6 days. The control data are the data for time zero. Within each column of the data, values with different superscript are significant at $p < 0.01$, with the same are not significant at $p > 0.05$ "nd", not detected.

Radiation treatment	UV-absorbing compounds/Chl *a* (μg/mg)		Car/Chl *a* (μg/μg)	
	3d	6d	3d	6d
Control	nd	nd	0.08 ± 0.01	0.08 ± 0.01
P	nd	0.18 ± 0.01[a]	0.29 ± 0.14	0.13 ± 0.00[a]
PA	nd	0.20 ± 0.02[a]	0.34 ± 0.14	0.11 ± 0.02[a]
PAB	0.65 ± 0.04	2.05 ± 0.01[b]	0.67 ± 0.10	0.77 ± 0.06[b]

than that under PA and P treatment (Table 1). This ratio showed higher values at day 3, however, it decreased with increased absorptivity of the UV-absorbing compounds.

4. Discussion

UVB-induced effects depend on many factors, such as the levels of irradiation, the sensitivity of the organisms, the spectral composition in the UV-B range and the exposure regime [32,9]. Although the radiation conditions used here can not replicate the natural solar conditions in the field, the results of the present study add to our knowledge in understanding the mechanisms involved in the inhibition and the photoprotective strategies developed in this red tide species during the prolonged UV exposure.

UV-B resulted in a continuous reduction of effective photosynthetic quantum yield of PSII (Fig. 3) and growth rate, while UV-A resulted much less inhibition. UV-B-related inhibition of PSII yield could be caused by damages to PSII proteins [33,34]. High UV-B exposures can also block the *de novo* synthesis of D1 protein, influencing the ability of cells to cope with the damage to PSII function [35]. In the absence of UV-B, UV-A or the higher level of PAR resulted in an initial decrease in the growth rate, which recovered later on (Fig. 1B). This initial decrease of growth was related to the initial decrease in photochemical activity of PSII (Fig. 3) and the metabolic cost for defending strategies against UVR. While the subsequent increase in growth rate indicates a physiological acclimation. Compared with PAR alone, presence of UV-A facilitated the recovery of growth in the late phase, as was supported by the negative inhibition of Φ_{PSII} caused by UV-A (Fig. 3B). Previous studies showed UV-A was involved in photorepair of damaged DNA [36] and used for CO_2 fixation by phytoplankton as an additional source of energy [7].

To minimize or counteract deleterious effects caused by short UV irradiances, phytoplankton cells often develop protective strategies, such as synthesis and accumulation of UV-absorbing compounds, which play a protective role against solar UVR [2]. In this study, presence of UV-B led to an induction of the UV-absorbing compounds in *S. costatum*. However, the concentration of UV-absorbing compounds peaked at 334 nm with the highest value of 2.05 μg mg^{-1} Chl *a* (equal to 2.1×10^{-9} μg $cell^{-1}$) was much lower than that of other red tide organisms, such as *Heterosigma akashiwo* and *Alexandrium tamarense*, that showed higher values $>4 \times 10^{-6}$ μg $cell^{-1}$ [5] and 14.5 μg μg^{-1} Chl *a* [37], respectively. Other studies on diatoms also showed lower levels of UV-absorbing compounds [38]. The low level of UV-absorbing compounds in *S. costatum*, together with the carotenoids which functioning as antioxidants and quenching photosensitization products [39], could not provide complete protection for *S. costatum* during the long-term exposure. For the cells exposed to PAR + UV-A, a very interesting protective strategy found: photoprotection was first activated with an increase in carotenoids, but was then an increase in the UV-absorbing compounds (Table 1). Such a temporal sequence, with changes in UV-absorbing compounds following changes in pigments, was also observed in a terrestrial cyanobacterium *Nostoc commune* [40]. Carotenoids might provide an immediate, active SOS response to counteract acute cell damage by UVR, but the dominating role in UV protection might still be played by UV-absorbing compounds, though its induction would take more time. However, a fast synthesis of UV-absorbing compounds would be operated when cells were confronted with huge potential damage, as seen here in cells exposed to high UV-B radiation in the presence of UV-A and PAR.

It was reported that cell enlargement could increase the pathlength of light traveling through the cell, thus afford greater protection to the nucleus of cells [41]. However, no pronounced increase in cell size was found in *S. costatum* in this study (Fig. 2). Cell volumes of diatom species have been shown to be increased when exposed to low or moderate level of UV-B radiation [9]. Both *Phaeodactylum tricornutum* [8] and *Cyclotella* sp. [9], when exposed to a low level of UV-B treatment (<2000 $Jm^{-2}\,d^{-1}$, DNA-weighted biologically effective dose), showed an increase of cell volume. However, higher UV-B treatment (3888 $Jm^{-2}\,d^{-1}$) used here might completely block the cellular metabolic processes, including protein and pigment biosynthesis, thus did not bring about significant change in the cell size of *S. costatum*.

In the oceanic environments, *S. costatum* cells are tossed up and down, receiving changing levels of UV radiation and PAR. Formation of *S. costatum* red tide depends on interactive effects of many environmental factors as well as on biological factors (such as grazing). However, the disappearance of the red tide might be more related to the organism's high sensitivity to solar UV-B, which caused more damages when the cells are distributed in the surface seawater during the blooms.

Acknowledgements

This research was supported by National Natural Science Foundation of China (Nos. 90411018; 40573059), Natural Science Foundation of Guangdong Province (No. 5300896).

References

[1] D.P. Häder, H.D. Kumar, R.C. Smith, R.C. Worrest, Effects of solar UV radiation on aquatic ecosystems and interactions with climate change, Photochem. Photobiol. Sci. 6 (2007) 267–285.
[2] R.P. Sinha, D.P. Häder, Life under solar UV radiation in aquatic organisms, Adv. Space Res. 30 (2002) 1547–1556.
[3] L.A. Franklin, P.J. Neale, Biological weighting function for the effect of UV radiation on carbon partitioning in microalgae, J. Phycol. 38 (2002) 10.
[4] S. Roy, B. Mohovic, S.M.F. Gianesella, I. Schloss, M. Ferrario, S. Demers, Effects of enhanced UV-B on pigment-based phytoplankton biomass and composition of mesocosm-enclosed natural marine communities from three latitudes, Photochem. Photobiol. 82 (2006) 909–922.
[5] K. Gao, W. Guan, E. Helbling, Effects of solar ultraviolet radiation on photosynthesis of the marine red tide alga *Heterosigma akashiwo* (Raphidophyceae), J. Photochem. Photobiol. B: Biol. 86 (2007) 140–148.
[6] E.W. Helbling, E.S. Barbieri, M.A. Marcoval, R.J. Gonçalves, V.E. Villafañe, Impact of solar ultraviolet radiation on marine phytoplankton of Patagonia, Argentina, Photochem. Photobiol. 81 (2005) 807–818.
[7] K. Gao, Y. Wu, G. Li, H.Y. Wu, V.E. Villafañe, E.W. Helbling, Solar UV radiation drives CO_2-fixation in marine phytoplankton: a double-edged sword, Plant Physiol. 144 (2007) 54–59.
[8] M.J. Behrenfeld, J.T. Hardy, H. Lee, Chronic effects of ultraviolet-B radiation on growth and cell volume of *Phaeodactylum tricorriutum* (Bacillariophyceae), J. Phycol. 28 (1992) 757–760.
[9] A.G.J. Buma, H.J. Zemmelink, K. Sjollema, W.W. C Gieskes, UVB radiation modifies protein and photosynthetic pigment content, volume and ultrastructure of marine diatoms, Mar. Ecol. Prog. Ser. 142 (1996) 47–54.
[10] K.I.M. Andreasson, S. Wängberg, Reduction in growth rate in *Phaeodactylum tricornutum* (Bacillariophyceae) and *Dunaliella tertiolecta* (Chlorophyceae) induced by UV-B radiation, J. Photochem. Photobiol. B: Biol. 86 (2007) 227–233.
[11] E.W. Helbling, B.E. Chalker, W.C. Dunlap, O. Holm-Hansen, V.E. Villafañe, Photoacclimation of antarctic marine diatoms to solar ultraviolet radiation, J. Exp. Mar. Biol. Ecol. 204 (1996) 85–101.

[12] L. Zudaire, S. Roy, Photoprotection and long-term acclimation to UV radiation in the marine diatom *Thalassionsira weissflogii*, J. Photochem. Photobiol. B: Biol. 62 (2001) 26–34.
[13] R.P. Sinha, A. Gröniger, M. Klisch, D.P. Häder, Ultraviolet-B radiation: photoprotection and repair in aquatic organisms, Recent Res. Develope. Photochem. Photobiol. 6 (2002) 107–119.
[14] A. Oren, N. Gunde-Cimerman, Mycosporines and mycosporine-like amino acids: UV protectants or multipurpose secondary metabolites?, FEMS Microbiol Lett. 269 (2007) 1–10.
[15] R. Alonso-Rodríguez, J.L. Ochoa, Hydrology of winter-sping "red tides" in Bahía de Mazatián, Sinaloa, México, Harmful Algae 3 (2004) 163–171.
[16] L. Ignatiades, O. Gotsis-Skretas, A. Metaxatos, Field and culture studies on the ecophysiology of the toxic dinoflagellate *Alexandrium minutum* (Halim) present in Greek coastal waters, Harmful Algae 6 (2007) 153–165.
[17] R.E. Korb, P.J. Saville, A.M. Johnston, J.A. Raven, Sources of inorganic carbon for photosynthesis by three species of marine diatom, J. Phycol. 33 (1997) 433–440.
[18] N.A. Nimer, M. Warren, M.J. Merrett, The regulation of photosynthetic rate and activation of extracellular carbonic anhydrase under CO_2-limiting conditions in the marine diatom *Skeletonema costatum*, Plant Cell Environ. 21 (1998) 805–812.
[19] L.A. Hobson, C.E. Hanson, C. Holeton, An ecological basis for extracellular carbonic anhydrase in marine unicellular algae, J. Phycol. 37 (2001) 717–723.
[20] X. Chen, K. Gao, Photosynthetic utilization of inorganic carbon and its regulation in the marine diatom *Skeletonema costatum*, Funct. Plant Biol. 31 (2004) 1027–1033.
[21] B. Rost, U. Riebesell, D. Sültemeyer, Carbon acquisition of marine phytoplankton: effect of photoperiod length, Limnol. Oceanogr. 51 (2006) 12–20.
[22] S.F. Wei, S.P.L. Hwang, J. Chang, Influence of ultraviolet radiation on the expression of proliferating cell nuclear antigen and DNA polymerase in *Skeletonema costatum* (Bacillariophyceae), J. Phycol. 40 (2004) 655–663.
[23] H. Cai, X. Tang, P. Zhang, Effects of UV-B radiation enhancement on DNA damage of three red-tide microalgae species, Chin. J. Appl. Ecol. 16 (2005) 559–562 (in Chinese).
[24] P. Zhang, X. Tang, S. Dong, H. Cai, H. Xaio, L. Feng, UV-B radiation plays different roles in the competition between *Alexandrium tamarense* and *Skeletonema costatum*, Oceanogr. Limnol. Sinica 38 (2007) 187–192 (in Chinese).
[25] W. Guan, K. Gao, Light histories influence the impacts of solar ultraviolet radiation on photosynthesis and growth in a marine diatom, *Skeletonema costatum*, J. Photochem. Photobiol. B: Biol. 91 (2008) 151–156.
[26] R.B. Setlow, The wavelengths in sunlight effective in producing skin cancer: a theoretical analysis, Proc. Natl. Acad. Sci. USA 71 (1974) 3363–3366.
[27] J.W. Rijstenbil, J.W.M. Derksen, L.J.A. Gerringa, T.C.W. Poortvliet, A. Sandee, M. Van Den Berg, J. Van Drie, J.A. Wijnholds, Oxidative stress induced by copper: defense and damage in the marine planktonic diatom *Ditylum brightwellii* (Grunow) West, grown in continuous cultures with high and low zinc levels, Mar. Biol. 119 (1994) 583–590.
[28] B.E. Genty, J.M. Briantais, N.R. Baker, Relative quantum efficiencies of the two photosystems of leaves in photorespiratory and non-photorespiratory conditions, Plant Physiol. Biochem. 28 (1989) 1–10.
[29] W.C. Dunlap, G.A. Rae, E.W. Helbling, V.E. Villafañe, O. Holm-Hansen, Ultraviolet-absorbing compounds in natural assemblages of Antarctic phytoplankton, Antarct. J. US 30 (1995) 323–326.
[30] S.W. Jeffrey, G.F. Humphrey, New spectrophotometric equations for determining chlorophylls a,b,c_1 and c_2 in higher plants, algae and natural phytoplankton, Biochem. Physiol. Pfl. 167 (1975) 191–194.
[31] T.R. Parsons, J.D.H. Strickland, Discussion of spectrophotometric determination of marine plant pigments, with revised equation for ascertaining chlorophylls and carotenoids, J. Mar. Res. 21 (1963) 155–163.
[32] R.C. Smith, B.B. Prézélin, K.S. Baker, R.R. Bidigare, N.P. Boucher, T. Coley, D. Karentz, S. Macintyre, H.A. Matlick, D. Menzies, M. Ondrusek, Z. Wan, K.J. Waters, Ozone depletion: ultraviolet radiation and phytoplankton biology in Antarctic waters, Science 255 (1992) 952–959.
[33] B. Demming-Adams, W.W. Adams, Photoprotection and other responses of plants to high light stress, Annu. Rev. Plant Physiol. 43 (1992) 599–626.
[34] J.N. Bouchard, D.A. Campbell, S. Roy, Effects of UV-B radiation on the D1 protein repair cycle of natural phytoplankton communities from three latitudes (Canada, Brazil, and Argentina), J. Phycol. 41 (2005) 273–286.
[35] Y. Nishiyama, S.I. Allakhverdiev, N. Murata, A new paradigm for the action of reactive oxygen species in the photoinhibition of photosystem II, Biochim. Biophys. Acta 1757 (2006) 742–749.
[36] A.G.J. Buma, P. Boelen, W.H. Jeffrey, UVR-induced DNA damage in aquatic organisms, in: E.W. Helbling, H.E. Zagarese (Eds.), UV Effects in Aquatic Organisms and Ecosystems Royal Society of Chemistry, Cambridge, UK, 2003, pp. 291–327.
[37] Laurion, F. Blouin, S. Roy, Packaging of mycosporine-like amino acids in dinoflagellates, Mar. Ecol. Prog. Ser. 279 (2004) 297–303.
[38] S.W. Jeffrey, H.S. MacTavish, W.C. Dunlap, M. Vesk, K. Groenewoud, Occurrence of UVA- and UVB-absorbing compounds in 152 species (206 strains) of marine microalgae, Mar. Ecol. Prog. Ser. 189 (1999) 35–51.
[39] S.B. Powles, Photoinhibition of photosynthesis induced by visible light, Ann. Rev. Plant Physiol. 35 (1984) 15–44.
[40] M. Ehling-Schulz, W. Bilger, S. Scherer, UV-B-induced synthesis of photoprotective pigments and extracellular polysaccharides in the terrestrial cyanobacterium *Nostoc commune*, J. Bacteriol. 179 (1997) 1940–1945.
[41] F. Garcia-Pichel, A model for internal self-shading in planktonic organisms and its implications for the usefulness of ultraviolet sunscreens, Limnol. Oceanogr. 39 (1994) 1704–1717.